

Multi-scale simulation of ductile iron casting

J Kubo

CAPCAST INC., 1-29-1, Gion, Shimotsukeshi, Tochigi 329-0434, Japan

Abstract. It has been well known that addition of rare earth elements was indispensable for production of ductile cast iron. The addition reduces solidification shrinkage. However there are still ambiguities in understanding the mechanism and predicting the casting defects. A possible explanation for the reduction of shrinkage is that the addition of rare earth promotes expansion of castings due to the graphite formation, which is related to cooling rate. In this study, the effect of rare earth addition was considered as a function of cooling rate and solidification shrinkage rate was determined by the macro-scale simulation. In the meso-scale and the micro-scale simulations, distribution of graphite nodules was compared with the experimental results. The multi-scale simulation result well reproduced the experimental results.

1. Introduction

Rare earth element is commonly added into the melt for production of ductile cast iron [1,2,3]. It is well realized that the resources of rare earth element are limited and the cost is relatively high, comparing to that of magnesium. It is of interest to know how the added rare earth elements influence the solidification structure, the defect formation (i.e. shrinkage defect) and consequently mechanical properties. One of the solutions is the prediction of the solidification structure including the casting defects by simulation in foundry. Since the addition of rare earth elements influences graphite nucleation and growth (micro-scale), interaction of graphite particles and dendrites (meso-scale) and shrinkage defect and residual stress (macro-scale).

This paper demonstrates an approach of multi-scale simulation using a commercial software code for predicting shrinkage defects. Figure 1 shows a conception for the multi-scale analysis for the cast iron in this study [4]. FEM [5] is used to know melt flow, solidification and stress in the macro-scale. In meso-scale, CAFE model which is originally developed by [6] is used to know microstructure and porosity. MCAFE model [7,8] is used to know dendritic structure in the micro-scale.

2. Macro-scale simulation predicting shrinkage defect by FEM mesh

2.1. Analysis model and conditions

The model used in the FEM analysis is shown in Figure 2. The mold is designed to produce two test pieces with 15 and 25 mm in thickness. The mesh size is approximately 3mm. A specimen which is equivalent to FCD 450 with the amount of rare earth (0.5% and 1.0%) is considered. It is assumed that molten cast iron (1350C) is assumed to be poured into mold.

In the model, the solidification shrinkage rate is treated as a function of cooling rate to represent the influence of rare earth elements on solidification manner. In general, volume of casting such as aluminium alloys and steel alloys monotonically shrinks during solidification. On the other hand, shrinkage of the ductile cast iron during solidifying is rather complicated. Due to volume expansion of graphite growth, the shrinkage depends on solidification condition. In this model, the influence of rare earth element addition and cooling rate is included by considering graphite nucleation.

In ductile cast iron, the following continuous equation is considered (Fig. 3) [9]. The first term corresponds to solidification shrinkage. It is generally negative, but the magnitude can be reduced by the graphite formation in the cast iron. The second term represents the melt flow in the mushy region



(interdendritic liquid metal feeding). The third term gives formation rate of shrinkage porosity. As a result, the shrinkage rate depends on the graphite growth.

$$\left(\frac{\rho_s}{\rho_L} - 1\right) \frac{\partial f_L}{\partial t} - \left(\frac{\partial f_L u}{\partial x} + \frac{\partial f_L v}{\partial y} + \frac{\partial f_L w}{\partial z}\right) + \frac{\partial f_v}{\partial t} = 0 \tag{1}$$

In the macro-scale simulation, test pieces with two different rare earth amount were analysed. The same parameters were used except the relationship between solidification shrinkage rate and cooling rate.

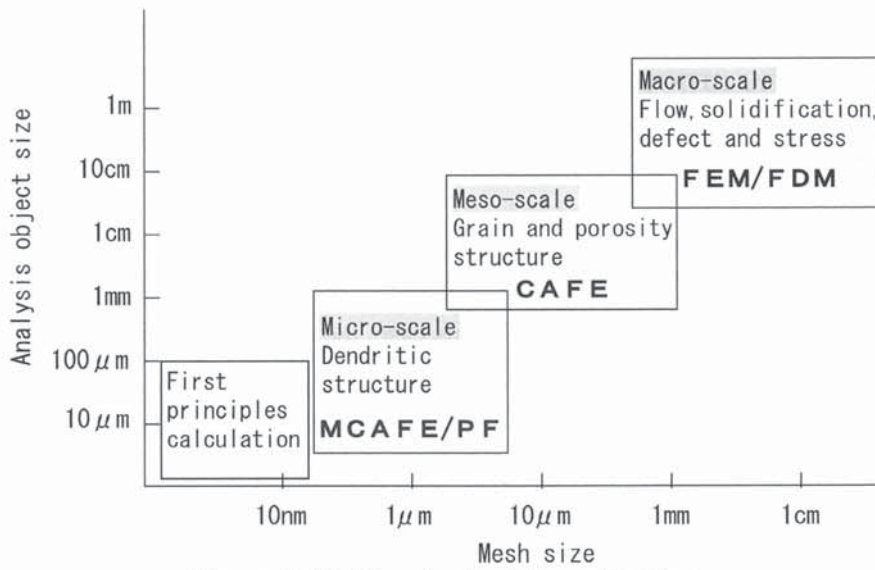


Figure 1. Multi-scale simulation of casting

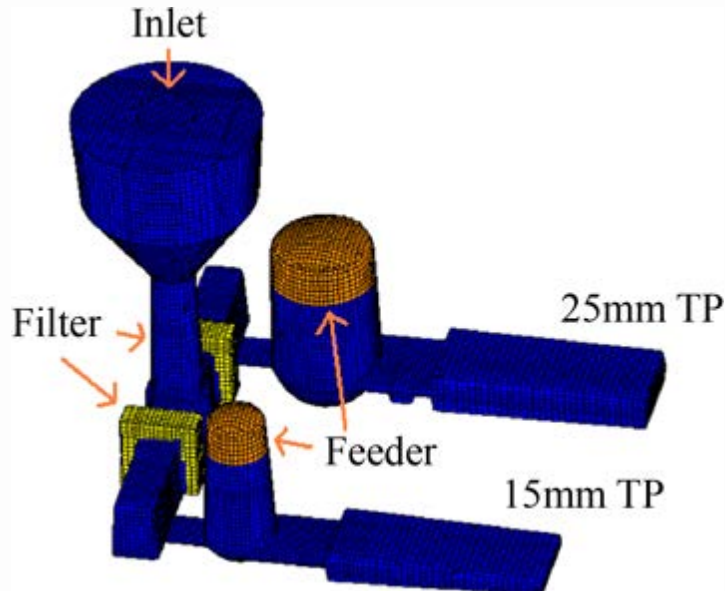


Figure 2. FEM mesh model

$$\underbrace{\left(\frac{\rho_S}{\rho_L} - 1\right) \frac{\partial f_L}{\partial t}}_{\textcircled{1}} - \underbrace{\left(\frac{\partial f_{Lu}}{\partial x} + \frac{\partial f_{Lv}}{\partial y} + \frac{\partial f_{Lw}}{\partial z}\right)}_{\textcircled{2}} + \underbrace{\frac{\partial f_v}{\partial t}}_{\textcircled{3}} = 0$$

- ① The amount of solidification shrinkage
- ② Interdendritic liquid metal feeding
- ③ The amount of porosity growth

Figure 3. Mechanism of shrinkage defect occurrence

2.2. Result and discussion

Figure 4 shows the longitudinal center section of test pieces of the experimental results and the calculated results. The predicted positions of the shrinkage defects essentially agree with those observed in the cast specimen. In the test piece of 15mm thickness, the shrinkage occurred near the feeder for 0.5% and 1% of rare earth content. In this case, the amount of rare earth elements up to 1% does not affect the position of the shrinkage defect.

In the test piece of 25mm thickness with 0.5% of rare earth elements, although the shrinkage defect in experimental specimen appears at the opposite side of feeder, the shrinkage defect is observed at the center. In the experimental specimen with 1.0% of rare earth elements, the shrinkage defect was completely avoided. The calculation also shows no shrinkage defect is produced in the test pieces. The experimental results clearly shows that the shrinkage defect is not likely to form with increasing amount of the rare earth elements. This tendency can be predicted by considering the influence of rare earth on the nucleation and growth of the graphite.

Quantitative comparison of the shrinkage defect volume between the experimental and the calculated results is shown in Figure 5. The volume of shrinkage defect in the experiments was measured by the Archimedes method. The calculated results qualitatively agree with the experimental results.

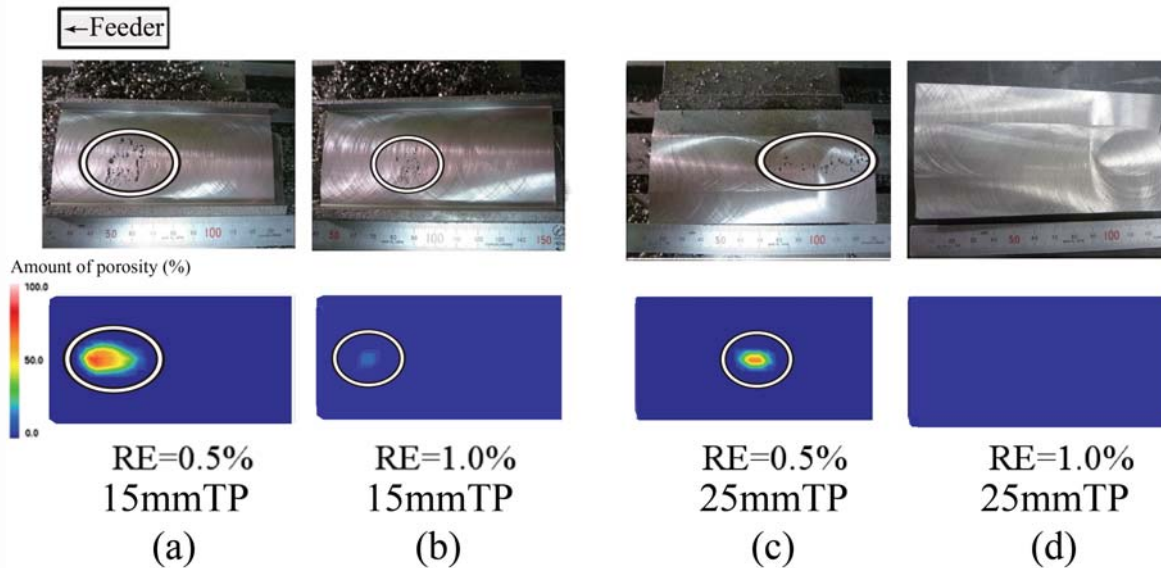


Figure 4. Comparison of shrinkage defects between macro-scale simulation and experiment. (a) 15mmTP RE=0.5%, (b) 15mmTP RE=1.0%, (c) 25mmTP RE=0.5%, (d) 25mmTP RE=1.0%.

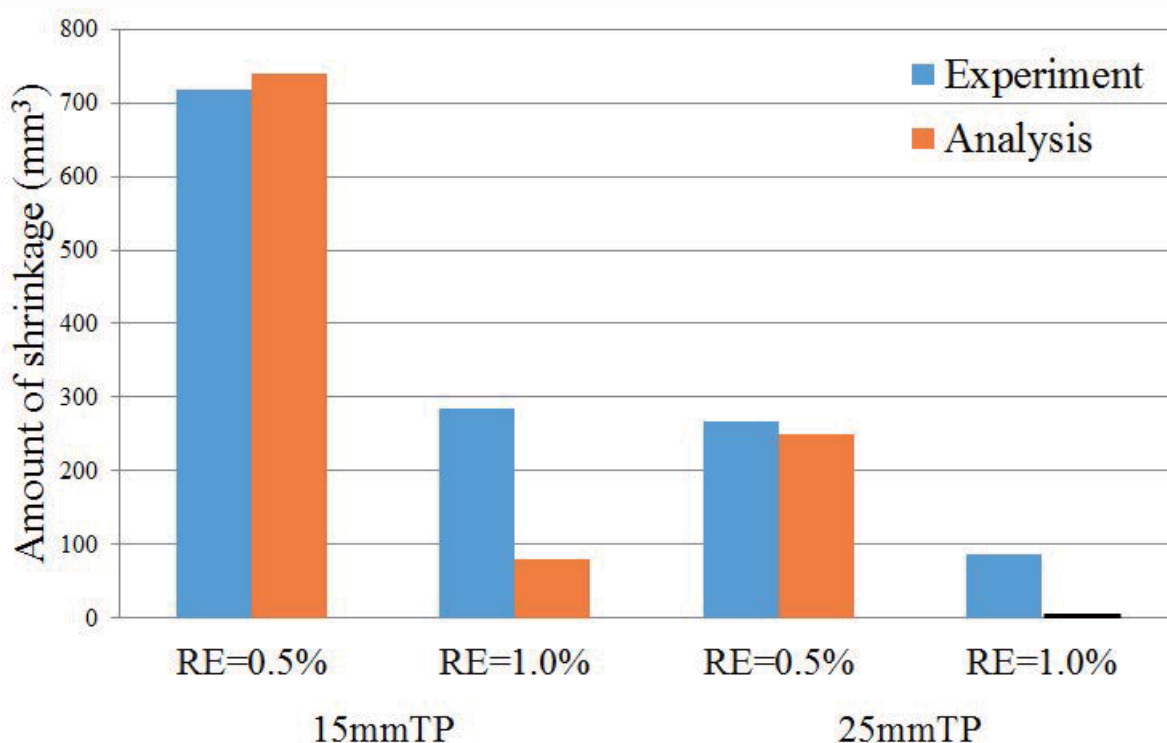


Figure 5. Comparison of shrinkage volume of test plates between simulation and experiment

3. Meso-scale simulation predicting shrinkage defect by CAFE method

3.1. Analysis model and conditions

In the meso-scale simulation, only two-dimensional model at the center section of the test pieces was analysed. The model was constructed by $200\ \mu\text{m}$ rectangular mesh. The grain structure was calculated by the CAFE method. In the calculation, the temperature profile, the solid fraction and the porosity volume, which was obtained by the macro-scale simulation, were introduced. The same parameters were used in CAFE model for the two different rare earth contents.

3.2. Result and discussion

Figure 6 shows comparison of the shrinkage defects with macro (grain) structure between the meso-scale simulation and the experiment. In the macro-scale simulation, the shrinkage defect was observed as the porosity distribution as shown in Figure 4. On the other hand, in the meso-scale calculation, shape and size of the shrinkage defect were indicated more precisely because $200\ \mu\text{m}$ rectangular mesh was small enough to represent shrinkage pore by vacant cells directly. Figure 6 shows the good agreement in the shape and size of the shrinkage defects between the calculated results and experimental one.

The positions of shrinkage are consistent from the macro-scale simulation to the meso-scale simulation. The effect of rare earth elements on the appearance of the shrinkage defects is also similar to that of the macro-scale calculation. Because the porosity volume calculated by the macro-scale calculation was distributed to the meso-scale cells, the vacant cells were produced at the same position.

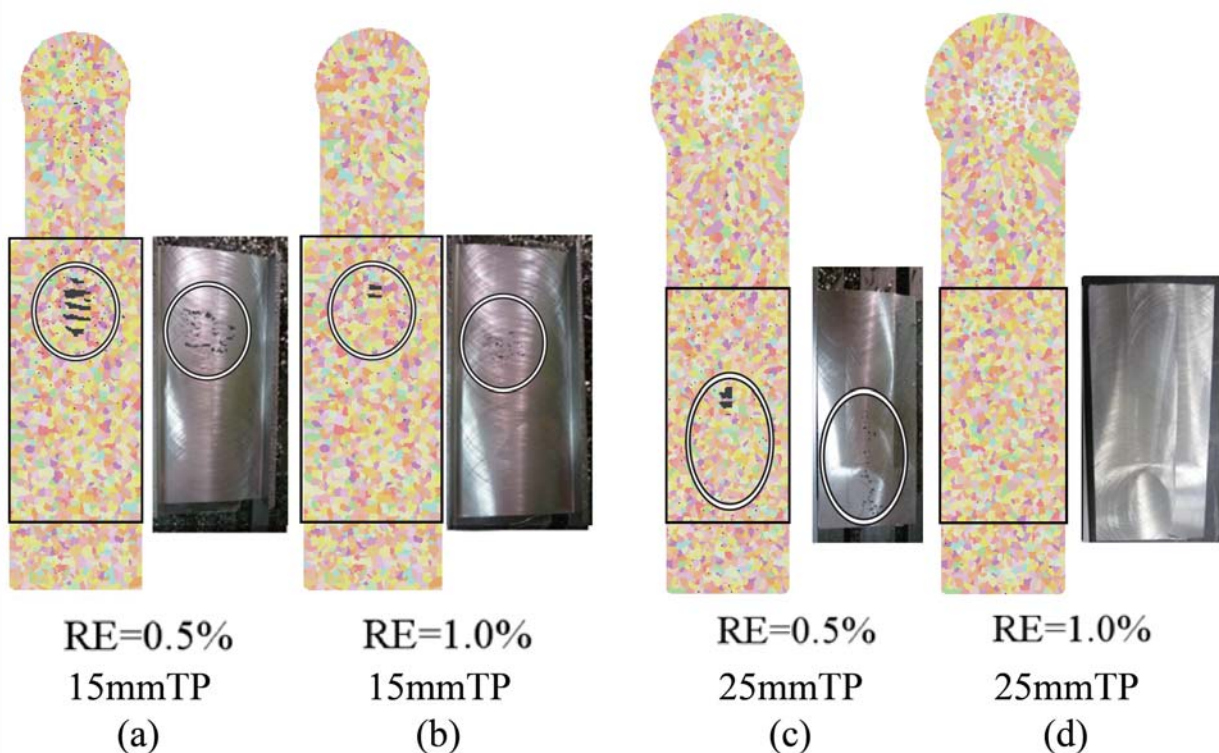


Figure 6. Comparison of shrinkage defects between meso-scale simulation and experiment. (a) 15mmTP RE=0.5%, (b) 15mmTP RE=1.0%, (c) 25mmTP RE=0.5%, (d) 25mmTP RE=1.0%.

4. Micro-scale simulation predicting micro structure by MCAFE

4.1. Analysis model and conditions

Location for the micro-scale simulation was 30mm from the tip of the plate, and the calculation domain was two-dimensional (1.3mm x 1.0mm). This model was constructed by $2\mu\text{m} \times 2\mu\text{m}$ rectangular meshes. This simulation was calculated by MCAFE method [8] using the temperature profile and the solid fraction obtained by the macro-scale simulation. Then the graphite nodule number was given by optimizing the parameters of the nucleation density of the graphite particles. The same parameters were used for the two different rare earth contents.

4.2. Result and discussion

Figure 7 compares the microstructure obtained by the MCAFE calculation with the microstructure obtained by the experiments. In order to analyze these results quantitatively, the images shown in Figure 7 were digitize. Then the number, average particle diameter and area ratio of the graphite nodules were measured by image processing. The number of graphite nodule in the test piece of 15mm thickness was larger than that in the test piece of 25mm thickness regardless of amount of rare earth. The reason is that the graphite nucleation frequency increases with increasing cooling rate. The test piece of 15mm thickness solidified earlier than 25mm thickness. Consequently the supercooling for the graphite nucleation in the test piece of 15mm thickness became larger and more nucleation of graphite nodule occurs. The average graphite nodule diameter in the test piece of 25mm thickness was larger than that in 15mm thickness. This tendency could be found in both the calculated result and the experimental one. The graphite area ratio ranged from 9 to 10% in both the calculated result and the experimental one. The graphite area ratio in the test piece of 25mm thickness was slightly larger than that in 15mm thickness.

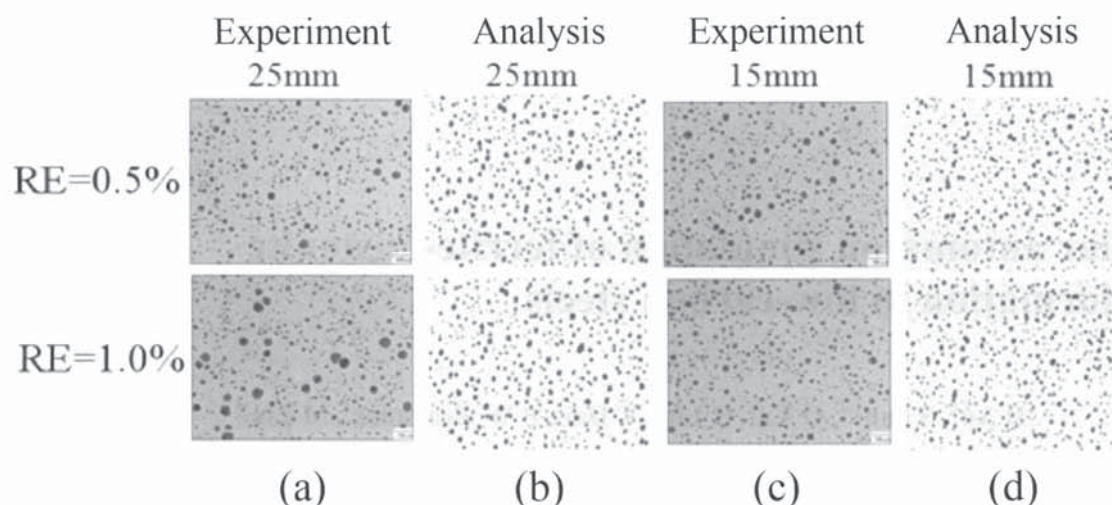


Figure 7. Comparison of micro structure between MCAFE simulation and experiment. (a) 25mm Experiment, (b) 25mm Analysis, (c) 15mm Experiment, (d) 15mm Analysis.

5. Conclusion

Multi-scale simulation for the plate ductile iron castings was performed. The results are summarized as follows:

- (1) Taking the effect of rare earth elements on the volume expansion due to the graphite formation into consideration, the shrinkage volume was calculated by the macro-scale simulation using FEM. In the test piece of 25mm thickness with addition of 1% of rare earth elements, no shrinkage defects were observed in both the simulation and the experiment. Amount of the shrinkage volume in the test pieces, obtained by the simulation is coincided well with the experimentally obtained value.
- (2) In the meso-scale simulation using CAFE method with $200\mu\text{m} \times 200\mu\text{m}$ rectangular meshes, the calculated results sufficiently reproduced shape and size of the shrinkage defects, comparing to the experimental results.
- (3) In the micro-scale simulation using MCAFE method with $2\mu\text{m} \times 2\mu\text{m}$ rectangular meshes, number density, mean diameter and area ratio of the graphite nodules coincided qualitatively with the experiment results.
- (4) On the basis of the macro-scale simulation, the meso-scale and the micro-scale simulations are useful for knowing the microstructure and the shrinkage defects in the ductile iron castings.

References

- [1] Morrogh H, Grant J W 1947 *J. Iron and Steel Inst.*, **155** 321
- [2] Gagnebin P A, Millis K D and Pilling N B 1949 *The Iron Age*, Feb., 77
- [3] Stefanescu D 1988 *ASM Handbook Volume 15: Casting*, ASM, Metals Park, Ohio
- [4] Kubo J, Okada K. 2013 *Japan Foundry Engineering Society 162nd Meeting* **5** 50
- [5] Kubo K, Deki N, Kubo J 2012 *13th World Conference on Investment Casting T7*
- [6] Rappaz M, Gandin Ch.-A 1993 *Acta Met. Mater.* **41** 345
- [7] M F Zhu, C P Hong 2001 *ISIJ Int.* **41** 436
- [8] Kubo K 2011 *Journal of Japan Foundry Engineering Society*, **83** 485, 533
- [9] Kubo K, Pehlke R D 1985 *Metallurgical Transactions* **16B** 359